RGNNV-induced cell cycle arrest at G1/S phase enhanced viral replication via p53-dependent pathway in GS cells

Weijun Mai*, Hongxiao Liu, Huiqing Chen, Yajing Zhou, Yan Chen

The Institute of Life Sciences, Jiangsu University, Zhenjiang, 212013, China

ABSTRACT

Nervous necrosis virus (NNV) is a ubiquitous pathogen in the aquaculture worldwide. Little is known about the relationship between NNV virus and host cells. Our studies showed that RGNNV infection could induce cell cycle arrest via activation of p53 signaling in cultured host cells. Infection of RGNNV redistributed NPM1, stabilized p53 and inhibited cell proliferation by inducing G1 arrest. RGNNV infection also led to phosphorylation and accumulation of p53 in a time-dependent manner. Furthermore, RGNNV infection upregulated cyclin-dependent kinase inhibitor 1 A (p21) and downregulated cyclin E and cyclin-dependent kinase 2 (CDK2). The expression of genes in the p53 pathway did not change significantly after p53 knockdown by pifithrin-α during RGNNV infection. However, NPM1 knockdown could abrogate RGNNV-induced cell proliferation inhibition, activation of p53 signaling and cell cycle arrest. In addition, RGNNV infection of the cells synchronized in various stages of cell cycle showed that viral genomic RNA and virus titer were higher in the cells released from G1 phase- or S phase-synchronized cells than that in the cells released from the G2 phase-synchronized or asynchronous cells after 18 h p.i. Therefore, our study reveals that RGNNV infection induces the p53-dependent pathway, resulting in a cell cycle arrest at G1 phase in host cells, which might provide a favorable condition for viral replication.

1. Introduction

Viral nervous necrosis (VNN) disease, induced by the nervous necrosis virus (NNV), has caused mass mortality in cultured marine fish at the larval stage, resulting in significant economical losses worldwide (Munday et al., 2002; Chi et al., 2003). However, the molecular mechanisms of NNV infection remain poorly understood. The NNV genome is composed of two positive single-stranded RNAs (RNA1 and RNA2) that lack poly-A tails. RNA1 encodes an RNA-dependent RNA polymerase (RdRp), and RNA2 encodes the capsid protein (Tan et al., 2001). A subgenome of RNA1, named RNA3, encodes the B1 and B2 proteins (Sommerset and Nerland, 2004). The B1 protein counteracts necrotic cell death by reducing mitochondrial membrane potential (MMP) loss, which in turn enhances cell viability (Chen et al., 2009). The B2 protein binds to newly synthesized viral double-stranded RNA, thereby preventing host RNA interference-mediated cleavage, and during the late stages of infection, can induce mitochondria-mediated cell death (Fenner et al., 2006; Su et al., 2014).

Viral infection could activate a variety of signal transduction pathways to induce subversion of the host cell cycle, which plays important roles in the viral life cycle by facilitating the replication of progeny virus after viral infection (Davy and Doorbar, 2007). Viral proteins have

been shown to block host DNA replication through cell cycle arrest in order to provide a favorable environment for viral DNA replication (Paladino et al., 2014). Many RNA viruses can induce G1, S or G2 arrest in infected cells to favor viral replication. For example, Human immunodeficiency virus (HIV)-infected T lymphocytes isolated from patients are arrested in G2 (Zimmerman et al., 2006); alphavirus M1 infection results in S phase accumulation of infected cells by down-regulating p21 proteion (He et al., 2010); Hepatitis C virus (HCV) NS2 protein induces cell cycle arrest in the S-phase in mammalian cells to facilitate HCV viral replication (Yang et al., 2006). Betanodavirus infection has been shown to alter some cell signaling pathways to maintain the cell viability during early infection in previous study (Low et al., 2017). However, the effects of NNV infection on the cell cycle of host cells and the significance of cell cycle regulation in NNV replication need to be further investigated.

The cell-cycle progression is tightly regulated through a complex network of cell-cycle regulatory molecules. Cyclin E-cdk2 complex and Cyclin D-cdk4 complex regulate cell cycle progression in the G1 phase. (Malumbres and Barbacid, 2009). These cell-cycle regulatory molecules have been found to be regulated by some upstream pathways such as p53 signaling. The protein p53 is stabilized and activated when a cell is exposed to stress conditions, i.e. genotoxic conditions, nucleolar stress

and/or viral infection, which leads to cell cycle arrest, apoptosis, DNA repair or senescence (El-Deiry, 1998). p53 signaling can regulate the expression of p21, which directly bind to some cdk-cyclin complexes to inhibit their kinases activity (He et al., 2005).

Nucleophosmin NPM1/b23 is a major multifunctional nucleolar phosphoprotein that plays a critical role in ribosome biogenesis (Lindström, 2010). Moreover, NPM1 participates in a variety of cellular activities including cell proliferation, cytoplasmic/nuclear shuttle transportation, transcriptional regulation and molecular chaperoning (Balusu et al., 2015). Recent studies have also highlighted that NPM1 has additional nonclassical roles, such as involvement in cell cycle regulation, cellular stress responses, and viral replication (Taoe et al., 2006). Most interestingly, NPM1 has been shown to shuttle molecules between the nucleolus and the cytoplasm, acting as a carrier protein for cell cycle-related protein p120, nucleolin, tumor suppressor ARF, p53, as well as several viral proteins such as the core protein of Hepatitis C virus, replication proteins of Adeno-associated virus and matrix protein of Newcastle disease virus (Mai et al., 2006; Bevington et al., 2007; Duan et al., 2014; Box et al., 2016). More specifically, several nucleolar proteins, including NPM1, nucleostemin and L5, interact with MDM2/p53 under stress conditions to inhibit its activity and stabilize p53 (Zhang and Lu, 2009). Furthermore, NPM1 has been shown to interact with HDM2, p53, and ARF, and can exert either a positive or negative influence on cellular growth by regulating the activities of these proteins (Tollini et al., 2011; Box et al., 2016).

In the present research, we investigate the effects of RGNNV infection on the cell growth and cell cycle of host cells, the roles of p53 signaling activation in regulation of cell cycle progression in RGNNV-infected cells, and the significance of cell cycle regulation in RGNNV replication. Furthermore, we also identify new functions of NPM1 in regulating the cell cycle via the p53 pathway as described in this study. Taken together, our results revealed that RGNNV infection could perturb the progression of cell cycle via the NPM1-p53 pathway and facilitate virus gene replication.

2. Materials and methods

2.1. Virus and cell culture

The RGNNV-C strain, isolated from NNV-infected grouper (*Epinephelus akaara*), was used in this study (Liu et al., 2012). The virus was proliferated in GS cells with a multiplicity of infection (MOI) of 1, after which infected cells were incubated at 28 °C in L-15 medium supplemented with 5% FBS and harvested when 90% of cells in the monolayer showed specific cytopathic effect (CPE). Virus titers determined by 50% tissue culture infective doses (TCID50) as described previously (Reed and Muench, 1938).

The GS cells (Qin et al., 2006) were derived from spleen tissue of the orange-spotted grouper (*Epinephelus coioides)* and cultured in Leibovitz's L15 medium supplemented with 5% fetal bovine serum (FBS) at 28 °C. Human H1299 cells were maintained in Dulbecco's modified Eagle's medium (DMEM, Gibco, Waltham, MA, USA) with 10% FBS and 1% penicillinand streptomycin (PS), and cultured in a humidified incubator with 5% CO_2 at 37 °C. Prior to infection or/and transfection, the plasmids or siRNA were mixed with Lipofectamine 2000 reagent (Invitrogen, Carlsbad, CA, USA) in Opti-MEM (Gibco, Waltham, MA, USA) and incubated for 20 min at room temperature. The Lipofectamine 2000-DNA complex was added to cells and mixed by gentle agitation. The growth medium (containing 5% or 10% FBS) was exchanged 6 h after infection or/and transfection.

2.2. Construction of plasmids

All his- and GST-tagged NPM1 and RGNNV capsid protein expression vectors were constructed as described previously (Mai et al., 2016). To generate a fusion protein of RGNNV capsid with green fluorescent

Table 1
Primers and siRNA sequences used in this study.

Primer name	Sequences (5'-3')
Capsid-HisF	CGGGGGATCCGACGATAGTCATGCCCCGCG
Capsid-HisR	CGAGCGGCCGCAAGCTTCCATGGTACGCAAAG
Capsid-GSTF	CGGGGGATCCACCATG GCTAGA GGTAAACAAAAT
Capsid-GSTR	CGAGCGGCCGCATTATTGCCGACGATAGCTCT
NPM1-HisF	GACGACAAG GGATCCAGAAGGTGCGTCCCTGCAT
NPM1-HisR	GCTC GCGGCCGC-CTGACAGCGCCTCCAACAC
NPM1-GSTF	GACGACAAG GGATCCGAAGATTCGGATGGACA
NPM1-GSTR	GCTC GCGGCCGCTTAAAGAGACTTCCTCCACTGC
P53-HisF	CGGGGGATCCGAAACAAACTGTATTGCCAGCTCTTG
P53-HisR	CGAGCGGCCGCGGTTCATGCCGCCCATGCAAACTGT
P53-GSTF	CGGGGGATCCACAACAAACTGTATTGCCAGCTCTTG
P53-GSTR	CGAGCGGCCGCAGGTTCATGCCGCCCATGCAAACTGT
Capsid-GFPF	CGGGGGATCCACCATG GCTAGA GGTAAACAAAAT
Capsid-GFPR	CGAGCGGCCGCATTATTGCCGACGATAGCTCT
B23-RT-F	TAAGGATCCTTAACCACCTTTTTCTATAC
B23-RT-R	GCCTAAGGATCCTTAGCCGGCAGCCGA
Capsid-RT-F	GCGCGTGCGACATGGTACGCAAAGGTGA
Capsid-RT-R	GCGCGCAAGCTTTTAGTTTTCCGAGTC
NNV-RT-F	CGCAAGGTTACCGTTTAGC
NNV-RT-R	GCATAAAGCTGACTAGGGGACCAAT
GADPH-RT-F	ATCACAGCCACACAGAAGACGG
GADPH-RT-R	CTTTCCCCACAGCCTTAGCAGC
B23-RNAi1	CAGUUUCACUAGGUGGAUUUGAGAU
B23-RNAi2	GAGCCAAAGACGAAUUACAUGUUGU
B23-RNAi3	CACCACCAUUUGUCUUGAGGUUAAA
Control siRNA	AUCUCAAAUCCACCUAGUGAAACUG

protein (GFP), the capsid ORF was subcloned into the XbaI and KpnI sites of the pcDNA3.1/CT-GFP-TOPO vector. GFP-capsid vector was produced and amplified in GS cells and the empty GFP vector was used as a control. The p53 open reading frame (ORF) was amplified by PCR using grouper *E.coioides* p53 cDNA (Genbank accession number HM622380.1) as the template, and then inserted into the pET28a and pGEX6p-1 vectors using specific primers (Table.1).

2.3. Antibodies

The following antibodies were used in the immunoprecipitation (IP) and Western blot (WB) analyses: capsid, NPM1 and GAPDH (as previously described by Mai et al., 2016); p53, phospho-p53(Ser15) and p21 (as previously described by Mai et al., 2012); MDM2 (N-20) (# sc-813, SantaCruz Biotechnology, Santa Cruz, CA, USA); cyclin E1 and CDK2 (Cell Signaling Technology, Danvers, MA, USA).

2.4. Real-time quantitative PCR analysis

SYBR green-based real-time PCR (Takara, Tokyo, Japan) was used to quantify RGNNV capsid protein expression levels. RNA concentrations in the samples were normalized based on expression of the housekeeping gene GAPDH. Table 1 lists the sequences of the primer sets that were used to amplify RGNNV capsid gene. RNA isolation and the real-time PCR operations were carried out according to Mai et al., 2016. The standard curve method was used to determine the fold-changes in RGNNV capsid gene mRNA expression levels. Quantitative analysis of viral genomic RNA (vRNA) from RGNNV-derived replicons was performed by real-time RT-PCR. The primers for qRT-PCR in this study were described in Table 1.

2.5. Cell proliferation and colony formation assays

Prior to the cell growth curve assay, the infected cells were seeded at 10^4 cells/well and grown in 24-well plates for 0–96 h in triplicates. The cells were harvested and counted at various pre-determined times. For cell viability assay, a modified MTT assay, performed according to the manufacturer's instructions (Promega, Madison, WI, USA) except

for the choice of medium, was used for the cell viability assay. Prior to the colony formation assay, the infected cells were sorted by luorescence-activated cell sorter (FACS), and 1000 cells were plated onto 6 cm dishes in triplicates. After culturing for 2–4 weeks, the cells were stained with 0.4% crystal violet (dissolved in 95% ethanol). The colonies were photographed and quantified to generate the presented histograms.

2.6. Flow cytometry analysis

Prior to the determination of cell cycle distribution, the infected or/ and transfected cells were grown until they achieved 30–40% confluence. The cells were then incubated in L15 medium at 28 °C for 6 h in the presence/absence of anti-p53 blocking antibody (30 ng/ml). The cells were then treated with 2 mM thymidine (Sigma Aldrich, St. Louis, MO, USA) for 12 h, after which they were transferred to growth medium for 10 h. This was followed by a secondary thymidine block of 12 h, after which the cells were transferred to growth medium. The cells were harvested at pre-determined times and then fixed with 70% cold ethanol and stained with 50 mg/ml propidiumiodide (Sigma, St Louis, Mo, USA), which was followed by RNase A (Sigma) treatment for 30 min at room temperature. DNA content was analyzed by a FACscan cell analyzer (BD Biosciences, San Jose, CA, USA) equipped with Cell quest software (BD Biosciences, San Jose, CA, USA). The population of cells in each phase was determined using ModFit LT software (BD Biosciences, San Jose, CA, USA).

2.7. Indirect immunofluorescence

The infected or/and transfected cells were seeded onto glass cover slips. Cells were washed with phosphate-bufferedsaline (PBS), fixed for 15 min in PBS containing 4% paraformaldehyde, and permeabilized in 0.5% Triton-X 100 in phosphate-buffered saline for 15 min at room temperature. Cells were then stained with specific antibodies for 1 h and washed extensively in PBS before being incubated with FITC-or TRITC-conjugated immunoglobulins for 1 h. Nuclei were counter-stained with DAPI. The images were acquired by confocal laser scanning microscopy (CLSM; LeicaTCS SP5, Leica, Wetzlan, Germany).

2.8. BrdU incorporation assays

Bromodeoxyuridine (BrdU) incorporation assays were conducted as described previously (Lee et al., 2016). After overnight starvation, the infected or/and transfected cells were pulsed with 10 mM BrdU (Sigma, St Louis, Mo, USA) for 10 h. The cells were then fixed in 4% paraformaldehyde and treated with 2 M HCl containing 1% Triton X-100. The cells were incubated with a monoclonal anti-BrdU (Sigma, St Louis, Mo, USA) antibody and then incubated with TRITC-conjugated goat anti-mouse antibody and stained with DAPI. A red immunofluorescence signal indicated BrdU in corporation. The total number of GFP-positive and BrdU-labeled cells was counted in 5–10 randomly selected areas of each dish.

2.9. RNAi-based NPM1 knockdown

The NPM1 short-interfering RNAs (NPM1-siRNAs), negative siRNA control (Cat.no.12935-400) and transfection reagents were purchased from Invitrogen. To study how NPM1 knockdown affects RGNNV infection in GS cells, the cells were transfected with NPM1 siRNAs using Lipofectamine PLUS (Invitrogen, Carlsbad, USA) for 5 h following the manufacturer's protocol and then infected with RGNNV (MOI = 1). The cultured cells were collected at pre-determined time points.

2.10. Western blot analyses

Protein extraction and western blot were performed as previously described (Dhar et al., 2006; Mai et al., 2016). Protein concentration was determined using a BCA Protein Assay Kit (Cowin Biotech, Beijing, China). Equivalent amounts of proteins were subjected to 12% sodium dodecyl sulfate-polyacrylamide gel electrophoresis and transferred to polyvinylidenedifluoride membranes (Millipore, Atlanta, GA, USA). The membranes were blocked for 2 h at 25 °C ± 2 °C in Tris-buffered saline containing 0.05% Tween® 20 and 5% nonfat milk, and incubated with specific primary antibodies raised against p53, phospho-p53(Ser15), MDM2, p21, cyclin E1, CDK2, capsid and GAPDH at 4 °C overnight, and with the corresponding secondary anti-rabbit or anti-mouse horse-radish peroxidase conjugated antibodies at appropriate dilutions for 1 h at 37 °C. Images were captured using a GeneGnome XRQ chemiluminescence detector (Syngene, Cambridge, UK); the densities of the protein bands were normalized to the GAPDH signal and quantified using GeneSys software (VilberLourmat, France). The abundance of the proteins of interest in the various treatments was expressed relative to the abundance under control conditions.

2.11. G1, S, and G2 synchronization in GS cells

GS cells were synchronized at G1 phase using serum deprivation by maintenance of cells in DMEM containing no FBS supplementation for 48 h. Synchronized cells were mock infected or infected with 1 MOI of RGNNV. After 1 h of virus adsorption, cells were treated with medium containing 5% FBS and harvested at various times post infection (p.i.) for cell cycle analysis. GS cells were synchronized at the S phase border using double-thymidine treatment by incubation for 12 h in maintenance media supplemented with 2 mM thymidine (Sigma, St Louis, Mo, USA). Cells were then washed three times with PBS and incubated for 10 h in maintenance media, followed by additional 12 h incubation in maintenance media supplemented with 2 mM thymidine. Then, synchronized cells were mock infected or infected with 1 MOI of RGNNV. GS cells were synchronized at G2 phase using nocodazole (Sigma, St Louis, Mo, USA) treatment by incubation of cells in maintenance media supplemented with 100 ng/ml nocodazole for 16 h. Cells were washed three times with PBS, and then infected with 1 MOI of RGNNV. At indicated times p.i., cells were processed for RT-PCR and flow cytometric analysis.

2.12. Statistical analysis

Data are mean ± SEM of three independent experiments. Results were analyzed by one-way analysis of variance (ANOVA). For each assay, student's *t*-test was used for statistical comparison. A value of P < 0.05 was considered significant.

3. Results

3.1. RGNNV induces nucleolar/ribosomal stress in GS cells

Previous data have shown both that NPM1 is a nucleolar/ribosomal stress-induced nucleolar protein and that the interaction between NPM1 and NNV capsid protein may represent a mechanism that is crucial to NNV infection (Mai et al., 2016; Yang et al., 2016). Thus, we hypothesized that RGNNV may induce nucleolar/ribosomal stress via NPM1. To test this hypothesis, we first confirmed that the GS cells had been effectively infected with RGNNV (Fig. 1A), after which the infection of RGNNV in GS cells was examined by RT-PCR (Fig. 1B, panel a) and Western blotting (Fig. 1B panel b). We could then investigate the expression levels of NPM1 and p53 in response to RGNNV infection. As shown in Fig. 1C, NPM1 was significantly upregulated in RGNNV-infected cells in a time-dependent manner (Fig. 1C, left panel). The expression of p53 also increased in these cells (Fig. 1C, middle). Fluor-ouracil (5-FU), which was used as a positive control, also induced NPM1 and p53 expression in a time-dependent manner (Fig. 1C, right panel). This chemotherapeutic agent inhibits ribosome biogenesis and
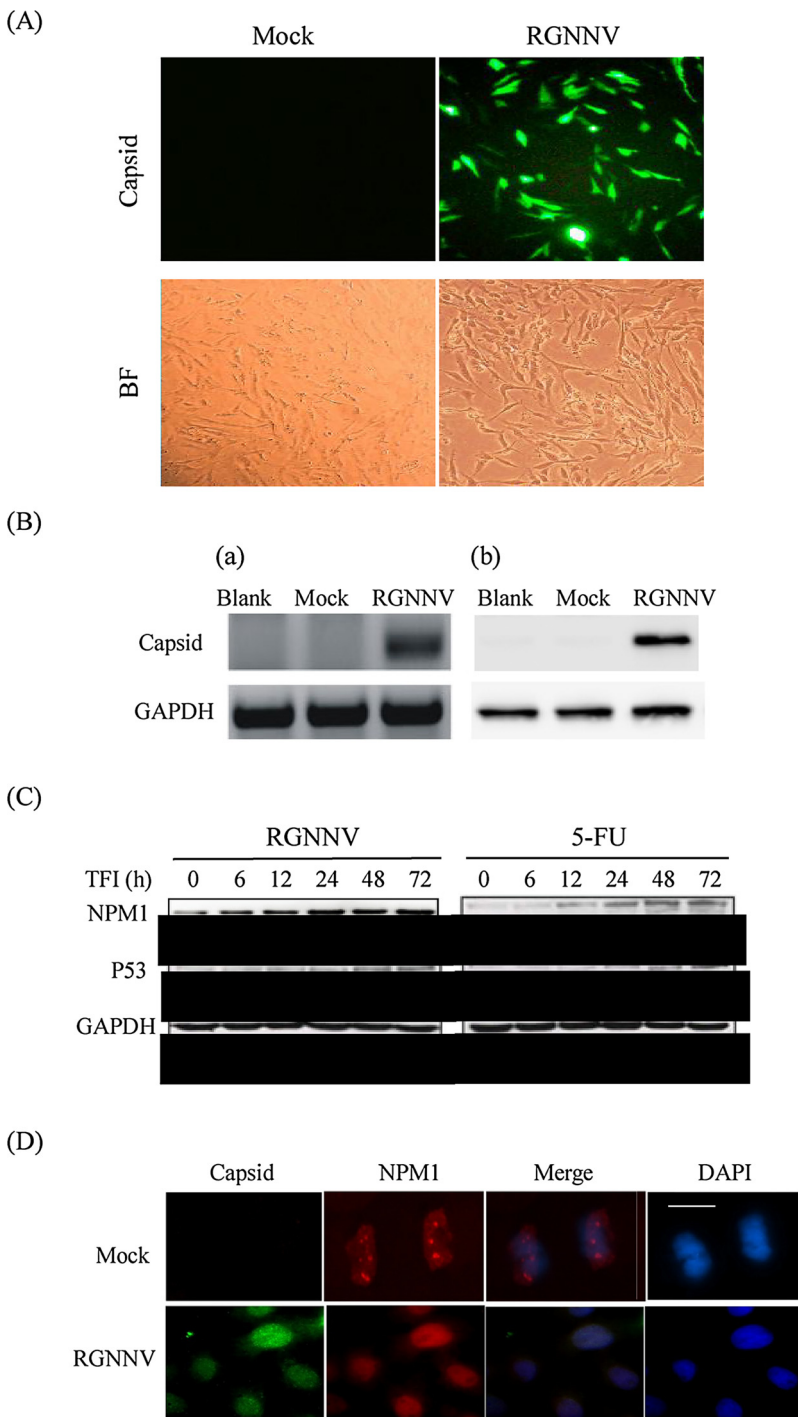
(A)

(B)

(C)

(D)

Fig. 1. **RG**NNV infection induces nucleolar stress. (A) GS cells were mock infected or infected with RGNNV. GS cells were mock infected or infected with 1 MOI of RGNNV, and the fluorescence images of RGNNV were examined by indirect fluorescence of capsid under a fluorescence microscope. BF: blank field, magnification: 9200. (B) Expression of RGNNV capsid in GS cells. Cells were mock infected or infected with 1 MOI of RGNNV for 24 h. Total RNA was isolated for RT-PCR analysis using specific primers for RGNNV capsid gene (left panel), and protein expression was determined by Western blotting with an anti-capsid antibody (K233) (right panel). Endogenous GAPDH expression was used as a loading control. (C) RGNNV infection induces NPM1 and p53 expression. GS cells were infected with RGNNV (MOI = 1) or treated with 5-FU for the indicated time periods. Cell lysates were then subjected to Western blotting to determine the expression of NPM1 and p53. The levels of the proteins at 0 h were considered 1-fold. (D) Subcellular localization of NPM1. Endogenous RGNNV capsid colocalizes with NPM1 in the whole cell and accumulates in the nucleus. Immunostaining of GS cells was performed with anti-capsid (green) and anti-NPM1 (red) antibodies. The nuclei were stained with DAPI. Bars, 20 μm (For interpretation of the references to color in this figure legend, the reader is referred to the web version of this article).

triggers nucleolar/ribosomal stress, which subsequently leads to p53 activation and cell growth arrest (Ghoshal and Jacob, 1994).

The redistribution of nucleolar proteins plays an important role in nucleolar/ribosomal stress response (Russo and Russo, 2017). GS cells infected RGNNV were fixed at 24 h and the intracellular localization of RGNNV capsid protein and NPM1 were examined by indirect immunofluorescence (Fig. 1D). NPM1 protein was distributed in nucleus in mock-infected GS cell. However, NPM1 protein exhibited diffuse cytoplasmic and nucleoplasmic distribution in addition to nucleolar accumulation, showing the same intracellular localization with RGNNV capsid in the GS cell.

Collectively, these results indicate that RGNNV infection might induce nucleolar/ribosomal stress and that NPM1 could play an important role in ribosomal stress response.

3.2. RGNNV infection inhibits GS cell proliferation and colony formation

Since RGNNV infection might induce nucleolar/ribosomal stress, we decided to investigate the additional consequences of RGNNV infection. The GS cells were mock infected or infected with RGNNV, and cell number was quantified at different time points to measure cell growth (Fig. 2A). The growth of cells infected with RGNNV was significantly inhibited in comparison to that of cells mock-infected. These results suggest that infection of RGNNV suppress cell proliferation. To confirm the inhibitory effect of RGNNV on cell proliferation, we performed MTS and colony formation assays in GS cells. As shown in both Fig. 2B and C,
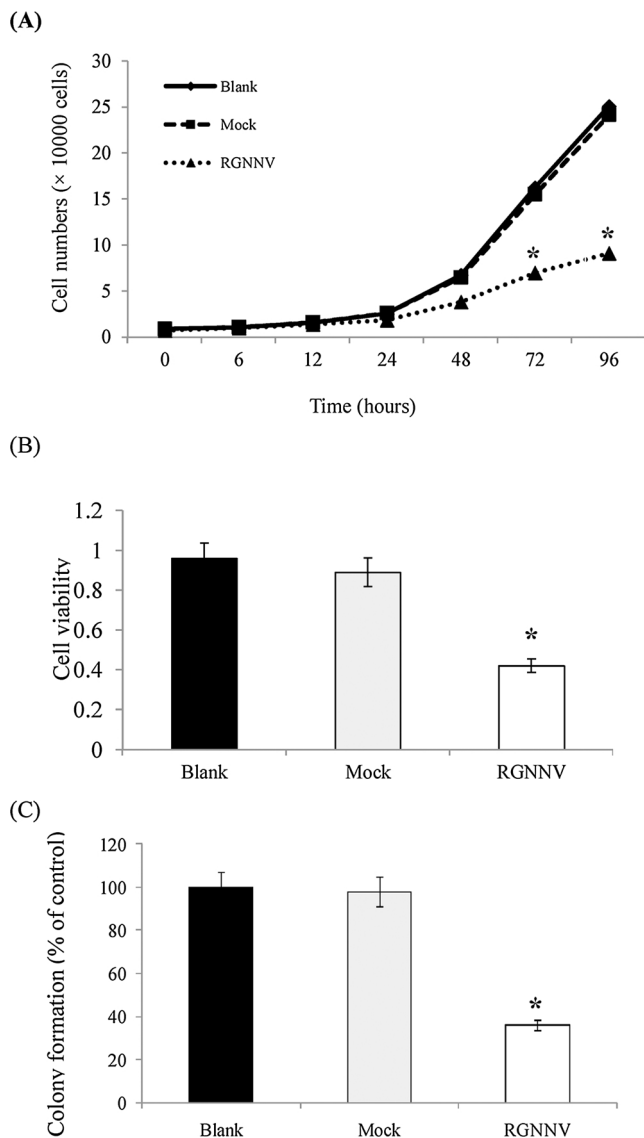
(A)

(B)

(C)

Fig. 2. Infection of RGNNV inhibits cell proliferation. (A) RGNNV infection inhibits GS cell proliferation. A total of 1.5×10^4 infected cells were seeded in 24-well plates and grown for 96 h with a quantification of cell number at dedicated times. (B) RGNNV infection reduces the number of viable GS cells. Equal numbers of cells infected with different constructs were seeded into a 96-well plate. After 72 h, the plate was subjected to a MTS assay. (C) Infection of RGNNV inhibits colony formation. Equal numbers of infected GS cells were seeded into 33-mm dishes. After a period of 96 h, the cells were stained with crystal violet. The percentage of colonies, in comparison to the control, is shown in (C). n = 3, * = P < 0.05.

RGNNV infection dramatically inhibited cell viability and colony formation whereas the control did not show any effect. These results demonstrate that RGNNV infection can inhibit cell proliferation.

3.3. Infection of RGNNV in GS cells inhibits DNA synthesis and arrests the cell cycle at the G1 phase

To gain more insight into how RGNNV infection inhibits cell proliferation in GS cells, we conducted 5-bromodeoxyuridine (BrdU) incorporation assays. RGNNV infection, when compared to the control, significantly reduced the number of BrdU positive cells (Fig. 3A and B), suggesting that RGNNV infection inhibits cell proliferation via reduced DNA synthesis.

To determine the effect of RGNNV infection on cell cycle

progression, we used FACS analysis to specify the cell cycle phases of cells RGNNV-infected or mock-infected. As shown in Fig. 3C, a significantly higher proportion of the cells infected with RGNNV, when compared to the control, were at the G1 phase ($\sim$71% compared to $\sim$ 48%) (Fig. 3C, left panel). Correspondingly, the percentage of cells in the S phase was markedly reduced in RGNNV-infected cells ($\sim$17%) in comparison to the control cells ($\sim$34%). To determine whether this RGNNV -induced cell cycle arrest is p53-dependent, the GS cells were mock infected or infected with RGNNV after which p53 was blocked by anti-p53 antibody. The FACS analysis demonstrated that the antibody-mediated blocking of p53 significantly reduced RGNNV-induced G1 arrest (Fig. 3C, right panel), indicating that the cell cycle progression effects of RGNNV are p53-dependent.

To further analyze the cell cycle progression in RGNNV-infected cells, the infected GS cells received double thymidine treatment, and were harvested at different time points after the thymidine had been removed from the culture medium. Cells RGNNV-infected or mock-infected both exhibited similar cell cycle distributions after thymidine treatment, indicating that the cells were similarly synchronized (Fig. 3D, time 0). However, a higher proportion of the cells infected with RGNNV were in the G1 phase in comparison to the control cells, particularly at the 4-h time point (Fig. 3D, 4 h). Hence, these results demonstrate that infection of RGNNV induces p53-dependent G1 delay.

3.4. Infection of RGNNV increases p53 levels and activity

To determine whether RGNNV infection induced p53-dependent G1 arrest by mediating p53 level and activity, we analyzed p53 levels after RGNNV infection in GS cells by immunofluorescence staining and Western blot analysis. RGNNV infection led to p53 accumulation in the nuclei when RFP fluorescence and specific anti-p53 antibody were used (Fig. 4A). Furthermore, the Western blot analyses show that RGNNV infection increased p53, MDM2, and p21 expression levels (Fig. 4B). In contrast, the mock-infected GS cells failed to induce p53 expression, as well as its target proteins (Fig. 4A and B). We then examined the half-life of p53 in RGNNV-infected or mock-infected GS cells by Western blot analysis to further investigate how RGNNV infection induces p53 expression. As shown in Fig. 4C, the half-life of the p53 protein was significantly extended to > 4 h in cells infected with RGNNV, which, when compared to the half an hour half-life in control cells (Fig. 4C), suggests that RGNNV infection stabilizes p53.

3.5. RGNNV induces cell cycle arrest via p53

Our results suggested that RGNNV infection induced phosphorylation of p53 (Ser15) and expression of p21. We treated cells with pifithrin-α (PFT-α), a specific inhibitor that blocks transcription of p53-responsive genes, to investigate the role of p53 in RGNNV-induced cell cycle arrest. We examined the levels of p53 and phospho-p53 (Ser15) in GS cells after PFT-α treatment. We found, by western blot, that treatment diminished p53 protein expression (Fig. 5, left panel). We also observed that pre-treatment of GS cells with PFT-α blocked the RGNNV-induced phosphorylation of p53 and expression of p21 (Fig. 5, middle panel). We also detected alterations to the levels of cyclin E and CDK2 in PFT-α treated cells (Fig. 5, middle panel) compared to the levels in infected cells without PFT-α treatment (Fig. 5, right panel).

Taken together, our findings demonstrated that RGNNV increased p53 signaling, leading to upregulation of p21 and concomitant downregulation of cyclin E and CDK2 in a time-dependent manner, resulting in cell cycle arrest at the G1 phase

3.6. NPM1 knockdown abrogates RGNNV-induced cell proliferation inhibition and cell cycle arrest

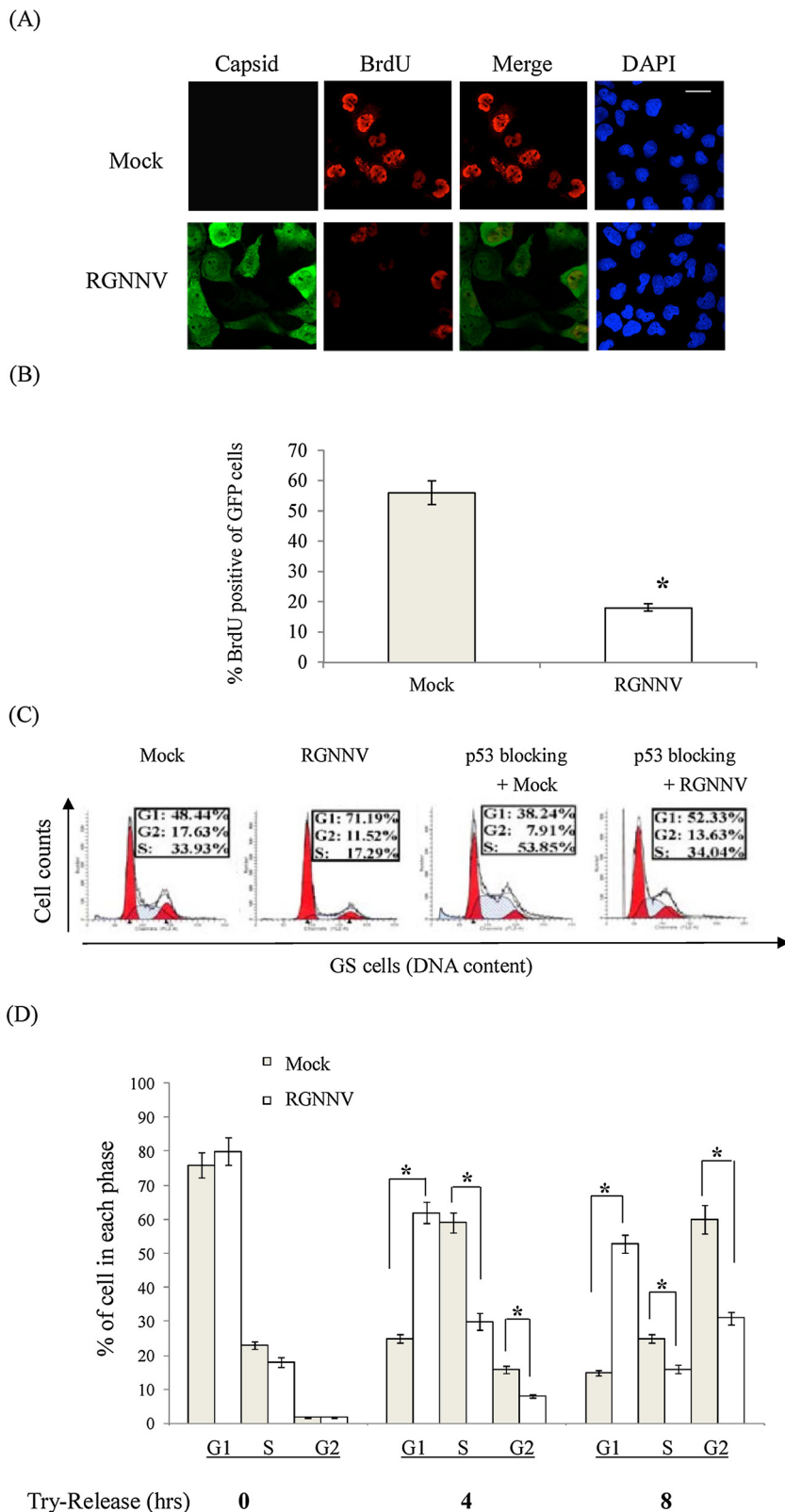As NNV capsid may interact with NPM1, which, when overexpressed, can activate p53 signaling and lead to growth arrest

(A)

(B)

(C)

GS cells (DNA content)

(D)

Try-Release (hrs)   0   4   8

Fig. 3. Infection of RGNNV inhibits BrdU incorporation and induces G1/S cell cycle arrest. (A) Infection of RGNNV inhibited BrdU incorporation. GS cells were mock infected or infected with 1 MOI of RGNNV, after which the cells were immunostained with a BrdU antibody (A). The percentage of BrdU positive cells in the GFP-labeled population (B) were determined as described in 'Materials and Methods' section. (C) Infection of RGNNV induces G1/S cell cycle delay. GS cells mock-infected or infected with 1 MOI of RGNNV were treated with and without a p53 antibody blocking, and the cells were then analyzed by FACS analysis. (D) Infection of RGNNV regulates G1/S phase transition in synchronized cells. The post-infected cells underwent a double-thymidine block, and the cells were then collected at the indicated time points. The cell cycle distributions of the cells were analyzed by FACS analysis. The error bars indicate the calculated standard deviations for three independent experiments, and the differences between mock-infection or infection with RGNNV were analyzed for statistical significance by Student's *t*-test. Thy: thymidine, * = $P < 0.05$. Bars, 20 μm.

(Colombo et al., 2002; Mai et al., 2016), we examined how alterations in NPM1 levels would affect cell cycle progression in RGNNV-infected GS cells. We first examined how low NPM1 levels would affect cell growth, as RGNNV infection was shown to induce NPM1 expression. The NPM1 levels were reduced to about a quarter of those in the control GS cells by siRNA transfection (Data not shown). Cell growth and MTS assays demonstrated that knockdown of endogenous NPM1 abrogated the cell proliferation inhibition witnessed in RGNNV-infected cells (Fig. 6A and B). Furthermore, FACS analysis and BrdU incorporation assays showed that NPM1 knockdown markedly attenuated the G1 arrest (Fig. 6C), and DNA synthesis reduction in RGNNV-infected cells (Fig. 6D). In contrast, nonspecific siRNA (control) did not significantly
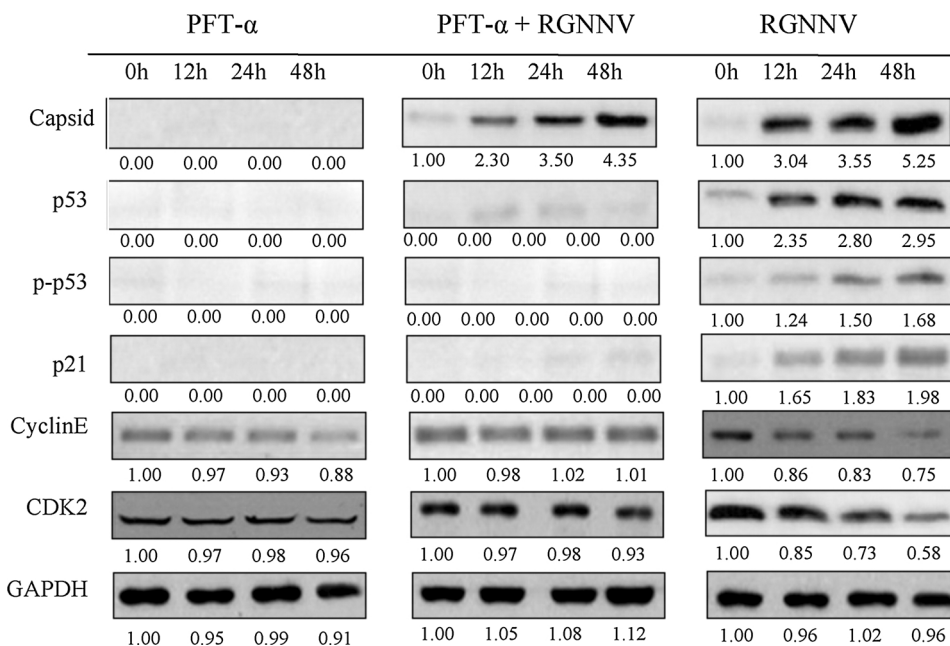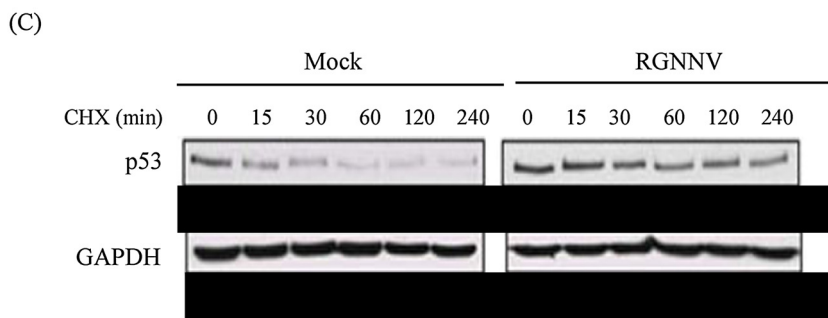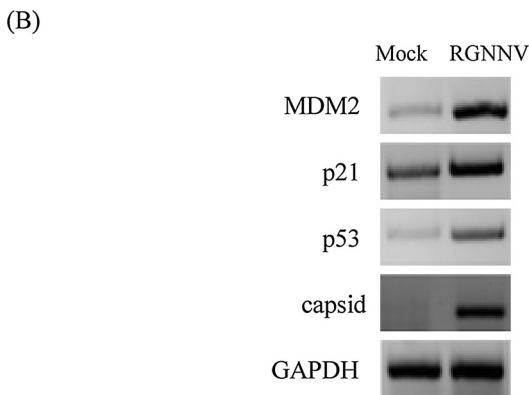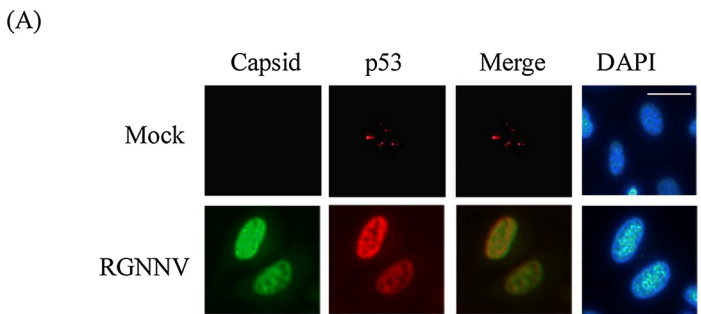
(A)

(B)

(C)

Fig. 4. RGNNV infection induces the accumulation of tumor suppressor p53. (A) RGNNV infection upregulates p53. GS cells were mock infected or infected with 1 MOI of RGNNV. Bars, 20 μm. (B) Infection of RGNNV regulates p53 downstream target proteins. GS cells were mock infected or infected with 1 MOI of RGNNV. Cell lysates were harvested and underwent 10% SDS-PAGE for Western blot analysis using antibodies specific for p53, p21, MDM2, capsid and GAPDH. (C) RGNNV infection stabilizes p53. GS cells were mock infected or infected with 1 MOI of RGNNV. for 48 h, after which the medium was supplemented with 50 μg/ml cycloheximide (CHX). The cells were harvested at the indicated time points and subjected to Western blot analysis with antibodies specific for p53 and GAPDH. The levels of the proteins at 0 h were considered 1-fold.

Fig. 5. Activation of p53 in RGNNV Shimen-infected macrophages is required for cell cycle arrest. To determine the effect of p53 in RGNNV-induced cell cycle arrest, p53 was depleted with the inhibitor PFT-α in RGNNV-infected and mock-infected GS cells. A significant reduction in p53 protein synthesis was detected in the presence of PFT-α (Lane 1 in the left panel and the middle panel). In the middle panel, pre-treatment of GS cells with PFT-α blocked RGNNV-induced phosphorylation of p53 and blocked the upregulation of p21. The levels of cyclin E and CDK2 were not reduced and no significant changes were observed in PFT-α-treated cells (middle panel), compared to RGNNV-infected cells without PFT-a treatment (the right panel). The levels of the proteins at 0 h were considered 1-fold.
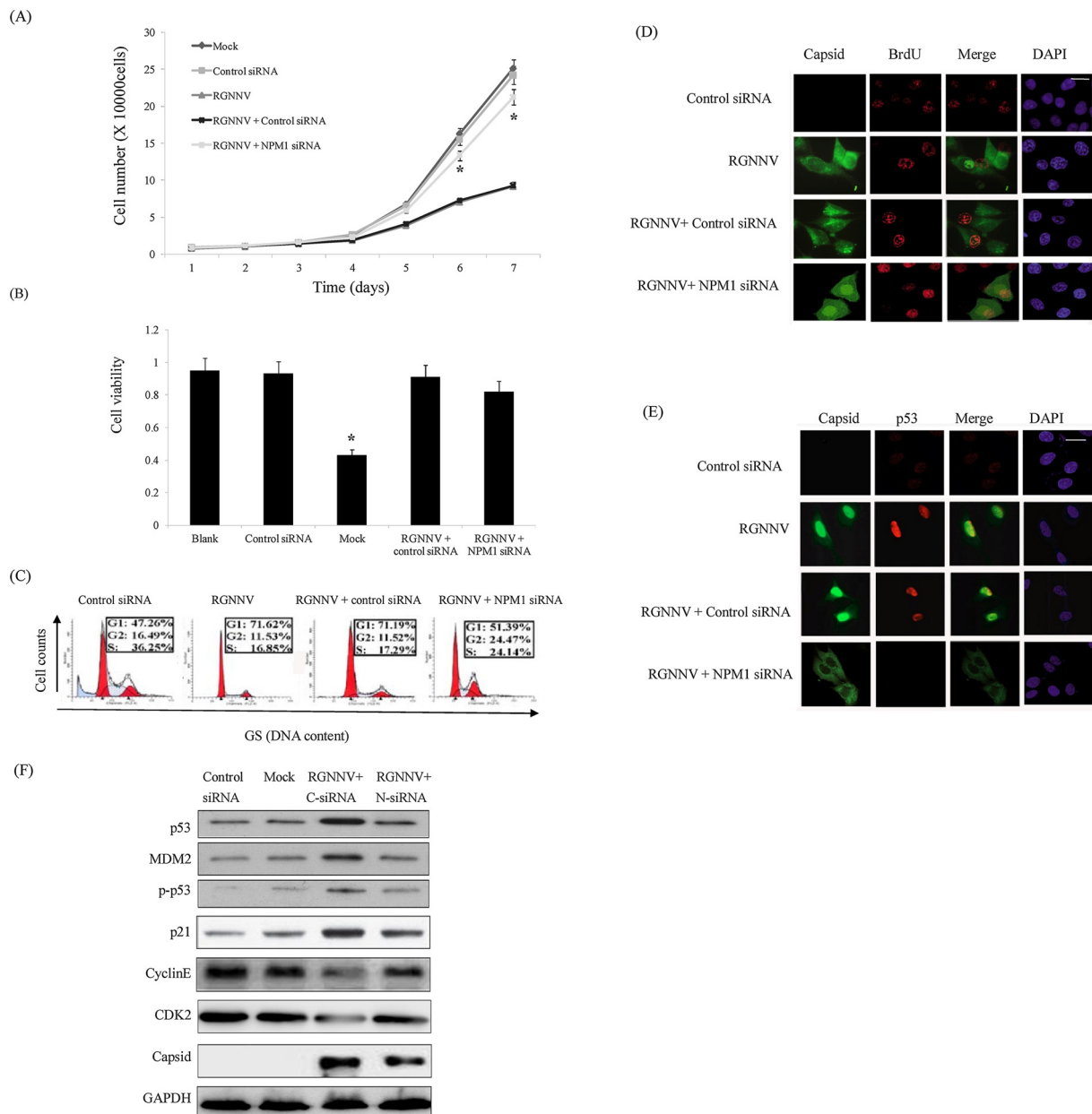
(A)

(B)

(C)

(D)

(E)

(F)

Fig. 6. NPM1 knockdown abrogates the RGNNV-induced inhibition of cell proliferation by activating p53. (A and B) NPM1 knockdown abrogates RGNNV-induced inhibition of cell growth and viability. Cell growth curves of GS cells (A), infected with RGNNV (MOI = 1) and/or siRNAs, determined for days 1–7 post-infection. Equal numbers of infected cells were seeded into 24-well plates and grown for 1–7 days with a quantification of cell number every day. The number of viable GS cells was measured by MTS (B). (C) NPM1 knockdown attenuates RGNNV-induced G1/S cell cycle delay. GS cells were infected with RGNNV (MOI = 1) and siRNAs for 48 h. Cell cycle distributions were analyzed by FACS analysis. (D) NPM1 knockdown reduces RGNNV-induced inhibition of BrdU incorporation. GS cells were infected with RGNNV (MOI = 1) and siRNAs for 48 h and then supplemented with BrdU. After 10 h, the cells were immunostained with a BrdU antibody (red) and the nuclei were stained with DAPI. (E) NPM1 knockdown regulates p53 protein levels. GS cells were infected with RGNNV and siRNAs for 48 h. Following immunostaining, GFP and p53 were detected with confocal laser scanning microscopy. (F) NPM1 downregulation decreased phosphorylation of p53 and its protein levels, as well as those of its target proteins, MDM2 and p21, cyclin E CDK2 and the RGNNV capsid protein. Bars, 20 μm (For interpretation of the references to color in this figure legend, the reader is referred to the web version of this article).

affect the RGNNV -induced cell growth inhibition and cell cycle arrest.

To determine whether NPM1 knockdown is associated with p53 pathway regulation, we examined p53 levels using immunofluorescence staining and Western blot analysis. As shown in Fig. 6E, p53 in both control cells and cells RGNNV-infected exhibited substantial nuclear accumulation. However, the RGNNV-infected cells that had been treated with NPM1 siRNA displayed only weak accumulation of endogenous p53 and its phosphorylation. Moreover, knockdown of endogenous NPM1 in the RGNNV-infected cells also decreased p21 and MDM2 levels then increased cyclin E and CDK2. In addition, the level of

RGNNV capsid level was lower in the NPM1-knockdowned cells than those in the control cells and RGNNV-infected cells (Fig. 6F). Taken together, these results indicate that the depletion of NPM1 dramatically decreased p53 activation and G1 arrest in cells with RGNNV infection which might affect viral replication.

3.7. Effects of cell cycle arrest at G1 phases on RGNNV replication

To investigate the effects of cell accumulation at G1 phases on RGNNV replication, synchronized cells in G1 phase, S phase, G2/M
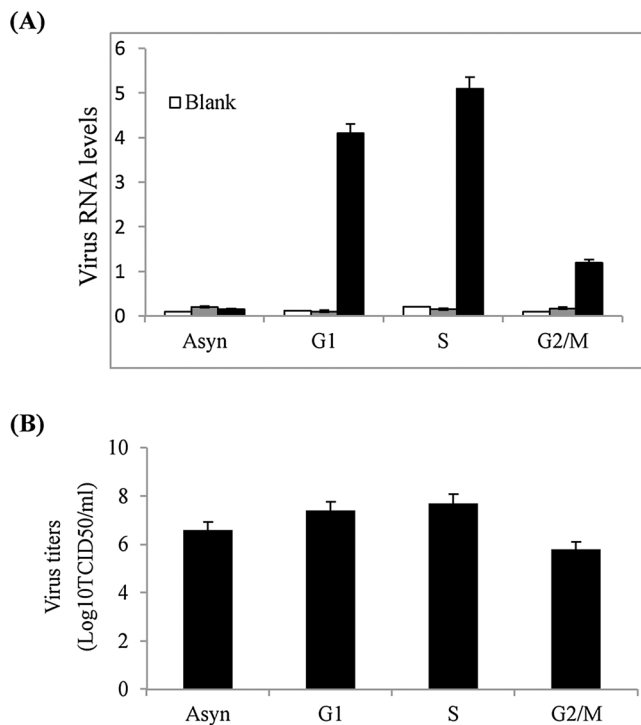
(A)

(B)

Fig. 7. Effects of cell cycle arrest at G1 and S phases on RGNNV replication. (A) RGNNV vRNAs levels. RGNNV vRNAs levels were determined at 18 h p.i. by qRT-PCR in the cells released from G1, S, G2-synchronized cells and asynchronous replicating cells. * = P < 0.05. (B) The titers of RGNNV in different treated cells. Total virus at 18 h p.i. was harvested by freezing and thawing cells three times and the viral titers were shown as log10TCID50/ml. Values are shown as the mean ± SEM. ** = P < 0.05.

phase or asynchronous cells were simultaneously released from their different phase of cell cycle, and then either mock infected or infected with 1 MOI of RGNNV, cell cycle profiles were determined by flow cytometry and RGNNV vRNA levels were determined by qRT-PCR at 18 h p.i. Results showed that the replication levels of vRNA were higher in the cells released from G1 or S-synchronized cells than that in the cells released from G2/M phase-synchronized or asynchronous cells (Fig. 7A). In addition, the titers of the virus also were higher in the cells released from G1 or S-synchronized cells than that in the cells released from G2/M phase-synchronized or asynchronous cells (Fig. 7B). These results suggest that RGNNV induction of host cell staying at G1 and S phase might be beneficial for virus replication.

4. Discussion

Previous research has highlighted that the nucleolus is a prime stress sensor of the cell, capable of activating cell cycle checkpoints in response to adverse conditions (Mayer and Grummt, 2005). Perturbations in nucleolar organization and/or function caused by viruses lead to reduced apoptosis, enhanced cell cycle progression and immune evasion. This allows viruses to hijack the host machinery to complete their life cycles (Hiscox, 2002). Furthermore, RNA viruses, whose primary site of replication is normally the cytoplasm, have also been characterized by cell cycle arrest of infected cells. Cell cycle manipulation is crucial event occurred in viruses-infected cells and many viruses employ a variety of mechanisms to utilize or manipulate the cell cycle pathways of infected cells (Davy and Doorbar, 2007; He et al., 2010). p53 is a key element in the induction of cell cycle arrest in viruses infected cells (Casavant et al., 2006). Some viruses interfere with the p53 surveillance pathways to promote replication (Rohaly et al., 2010; Luo et al., 2011), other viruses exhibited a p53-independent way for its replication (Dahl et al., 2005; Kucharski et al.,

2011). The first transcriptional target of p53 was p21, which bridges the function of p53 with the cell cycle and plays important roles in regulation of cell cycle progression or arrest (He et al., 2005). In this study, we focused on whether the p53 signaling pathway contributes to RGNNV induced cell cycle progression and virus replication. Our studies have demonstrated that RGNNV infection induced the activation of p53 signaling pathway to up-regulate p21 and down-regulate cyclin E and CDK2, forcing the infected cells to stay in the replicative G1/S phase.

Some viruses can regulate the cell cycle progression through interaction between virus and host cells in order to induce the cell cycle arrest and provide an advantageous environment for viral replication (Dove et al., 2006; Li et al., 2007). Infectious bronchitis virus (IBV) induces an S and G2/M-phase arrest to favor viral replication (Dove et al., 2006; Li et al., 2007), and mouse hepatitis virus (MHV) (Chen and Makino, 2004) and some severe acute respiratory syndrome coronavirus (SARS-CoV) proteins induce cell cycle arrest in G1 phase (Yuan et al., 2006). We found that the infection of RGNNV in the GS cell line induced nucleolar/ribosomal stress, inhibited cell proliferation and induced cell cycle arrest at the G1 phase. To specifically investigate whether a particular stage of the cell cycle favored RGNNV replication, we synchronized cells in various stages of the cell cycle and compared efficiencies of virus infection. Results showed that RGNNV replication levels, sgRNA synthesis were greater in the cells released from G1 phase or S phase of the cell cycle after 18 h p.i., when compared to either cells released from the G2 phase or asynchronous cells. Our results also provided evidences that RGNNV titer in the cells released from G1 phase or S phase synchronized cells was higher than that in cells released from G2/M phase synchronized cells. This might be that cells synchronized at G2/M phase need longer time to reenter cell cycle progression than synchronized cells at the G1 or S phase, which support the hypothesis that S phase state was beneficial for virus replication. Therefore, we favor the hypothesis that RGNNV induces G1 phase cell cycle arrest in order to provide a more favorable condition for virus production.

The p53 signaling pathway plays an important role in the induction of cell cycle arrest in virus infected cells (Casavant et al., 2006). Viruses activate or interfere with the p53 signaling pathway at different levels to achieve proliferation. As a DNA damage response protein, p53 transcriptionally activates numerous genes involved in DNA repair and cell cycle arrest (Malunber and Barbacid, 2009), and p53-dependent arrest of cells at G1/S or G2/M phase is an important component of the cellular response to genotoxic stress including virus infection (Casavant et al., 2006; Luo et al., 2011). The reported researches are beneficial to a deep-going understanding to the activation of p53 signaling pathway by RGNNV. Our observations were consistent with those in a previous report (Laptenko and Prives, 2006), which suggested that activation of p53 causes accumulation of p21, a cyclin-dependent kinase inhibitor, and eventual induction of downstream target genes such as cyclin E and CDK2. Both p21 and p53 cause cell cycle arrest at the G1 checkpoint, which promotes DNA repair by allowing sufficient time for damaged DNA to be repaired before it is passed to daughter cells (He et al., 2005; Rohaly et al., 2010). The main target of p21 is the cyclin E-CDK2 complex, in addition to the cyclin D-CDK4/6 complex (Roberts and Sherr, 2003). The Cyclin E-CDK2 complex is inhibited by p21 during the progression from G1 to S phase (Möröy and Geisen, 2004). Cells regulate the p53 pathway, which controls the cell cycle, in order to maintain their stability and modulate their differentiation (Vogelstein et al., 2000). Researchers are investigating the infection strategies that facilitate viral proliferation by manipulating the cell cycle. It is possible that G1/S phase arrest may aid viral replication through an increase in critical cellular materials (nucleotide, amino acid, or lipid) (Baer et al., 2012). In this study, we showed that RGNNV infection induced p53 and p21 accumulation, phosphorylation of p53 (Ser15) and cyclin E-CDK2 decrease. Furthermore, PFT-α, a specific inhibitor of p53, prevented the arrest of the cell cycle in RGNNV-infected cells. Thus, infection with

RGNNV activated p53, resulting in upregulation of p21, inhibition of cyclin E-CDK2, and, ultimately, cell cycle arrest, which could facilitate virus gene replication. This observation is not consistent with the findings in other RNA virus, which induced cell cycle arrest at both S and G2/M phases independent of p53 (Li et al., 2007), suggesting that p53 might play different roles in RNA viruses-infected cells.

We previously showed that NPM1 interacts with RGNNV capsid to enhance RGNNV replication (Mai et al., 2016). However, the physiological function of this evolutionarily conserved protein in RGNNV infection remains obscure. In the current study, we showed that NPM1 is mainly localized to the nucleolus, but that some can also exist in the nucleus and cytoplasm. NPM1 expression was induced when cells were infected with RGNNV. Interestingly, the knockdown of endogenous NPM1 abrogated RGNNV-induced G1 arrest and cell proliferation inhibition via a p53-dependent pathway. Several proteins that impact cell survival by interacting with, and regulating, NPM1 protein levels have been identified. After various stimuli, NPM1 releases ARF, which allows binding to MDM2 and the prevention of proteasomal degradation of p53. These observations provide evidence that NPM1 regulates cell fate in a p53-dependent manner by directing ARF to the nucleolus and preventing inhibition of MDM2 (Korgaonkar et al., 2005; Qin et al., 2011). Other studies have also linked NPM1 with the tumor suppressor activity of p53. For example, NPM1 is able to interact directly with MDM2, independently of ARF, to inhibit p53/MDM2 and protect p53 from degradation (Kurki et al., 2004). Moreover, NPM1 has also been reported to directly associate with p53 for p53 stabilization and activation (Lambert and Buckle, 2006; Russo and Russo, 2017). We observed that NPM1 and p53 levels increased following the ribosomal stress caused by RGNNV infection. This observation led us to hypothesize that NPM1 can respond to ribosomal stress and regulate cell proliferation. However, the exact mechanism through which NPM1 exerts this function remains unclear. Earlier research in cells exposed to ionizing radiation and polyamine depletion has shown that NPM1 may function as a negative regulator for the p53/MDM2 interaction, which would lead to the stabilization of p53 (Zou et al., 2005). NPM1 may also function similarly to the molecular chaperone Hsp90 (Muller et al., 2004), which prevent self-aggregation and degradation, facilitate protein complex formation and/or monitors trafficking and correct cellular localization.

In conclusion, our research reveals that infection of RGNNV can activate p53-dependent pathway, resulting in G1/S phase cell cycle arrest in host cells and directly impacting viral replication. Furthermore, our study also shows that NPM1 might is a new regulator of the p53 pathway potentially in response to RGNNV infection. Our finding that RGNNV has the potential to suppress host cell growth in a p53-dependent manner has important implications for NNV pathogenesis studies. However, a detailed mechanism of how RGNNV, along with factors that mediate regulatory pathways, induces cell cycle arrest at the G1 phase is not completely available, and should be clarified by future research.

References

Baer, A., Austin, D., Narayanan, A., Popova, T., Kainulainen, M., Bailey, C., 2012. Induction of DNA damage signaling upon rift valley fever virus infection results in cell cycle arrest and increased viral replication. J. Biol. Chem. 287, 7399.

Balusu, R., Fiskus, W., Bhalla, K.N., 2015. Nucleophosmin (NPM1) Targeted Therapy of Acute Myeloid Leukemia. Springer, New York, pp. 251–273.

Bevington, J.M., Needham, P.G., Verrill, K.C., Collaco, R.F., Basrur, V., Trempe, J.P., 2007. Adeno-associated virus interactions with B23/Nucleophosmin: identification of sub-nucleolar virion regions. Virology 357, 102–113.

Box, J.K., Paquet, N., Adams, M.N., Boucher, D., Bolderson, E., O'Byrne, K.J., Richard, D.J., 2016. Nucleophosmin: from structure and function to disease development. BMC Mol. Biol. 17, 19.

Casavant, N.C., Luo, M.H., Rosenke, K., Winegardner, T., Zurawska, A., Fortunato, E.A., 2006. Potential role for p53 in the permissive life cycle of human cytomegalovirus. J. Virol. 17, 8390–8401.

Chen, C.J., Makino, S., 2004. Murine coronavirus replication induces cell cycle arrest in G0/G1 phase. J. Virol. 78, 5658–5669.

Chen, L.J., Su, Y.C., Hong, J.R., 2009. Betanodavirus non-structural protein B1: a novel anti-necrotic death factor that modulates cell death in early replication cycle in fish cells. Virology 385, 444–454.

Chi, S.C., Shieh, J.R., Lin, S.J., 2003. Genetic and antigenic analysis of betanodaviruses isolated from aquatic organisms in Taiwan. Dis. Aquat. Organ. 55, 221–228.

Colombo, E., Marine, J.C., Danovi, D., Falini, B., Pelicci, P.G., 2002. Nucleophosmin regulates the stability and transcriptional activity of p53. Nat. Cell Biol. 4, 529–533.

Dahl, J., You, J., Benjamin, T.L., 2005. Induction and utilization of an ATM signaling pathway by polyomavirus. J. Virol. 79, 13007–13017.

Davy, C., Doorbar, J., 2007. G2/M cell cycle arrest in the life cycle of viruses. Virology 368, 219–226.

Dhar, S.K., Xu, Y., Chen, Y., Clair, D.K.S., 2006. Specificity protein 1-dependent p53-mediated suppression of human manganese superoxide dismutase gene expression. J. Biol. Chem. 281, 21698–21709.

Dove, B., Brooks, G., Bicknell, K., Wurm, T., Hiscox, J.A., 2006. Cell cycle perturbations induced by infection with the coronavirus infectious bronchitis virus and their effect on virus replication. J. Virol. 80, 4147–4156.

Duan, Z., Chen, J., Xu, H., Zhu, J., Li, Q., He, L., Liu, H., Hu, S., Liu, X., 2014. The nucleolar phosphoprotein B23 targets Newcastle disease virus matrix protein to the nucleoli and facilitates viral replication. Virology 452–453, 212–222.

El-Deiry, W.S., 1998. Regulation of p53 downstream genes. Semin. Cancer Biol. 8, 345–357.

Fenner, B.J., Thiagarajan, R., Chua, H.K., Kwang, J., 2006. Betanodavirus B2 is an RNA interference antagonist that facilitates intracellular viral RNA accumulation. J. Virol. 80, 85–94.

Ghoshal, K., Jacob, S.T., 1994. Specific inhibition of pre-ribosomal RNA processing in extracts from the lymphosarcoma cells treated with 5-fluorouracil. Cancer Res. 54, 632–636.

He, G., Siddik, Z.H., Huang, Z., Wang, R., Koomen, J., Kobayashi, R., Khokhar, A.R., Kuang, J., 2005. Induction of p21 by p53 following DNA damage inhibits both Cdk4 and Cdk2 activities. Oncogene 24, 2929–2943.

He, Y., Xu, K., Keiner, B., Zhou, J., Czudai, V., Li, T., Chen, Z., Liu, J., Klenk, H.D., Shu, Y.L., 2010. Influenza A virus replication induces cell cycle arrest in G0/G1 phase. J. Virol. 84, 12832–12840.

Hiscox, J.A., 2002. The nucleolus–a gateway to viral infection? Arch. Virol. 147, 1077–1089.

Korgaonkar, C., Hagen, J., Tompkins, V., Frazier, A.A., Allamargot, C., Quelle, F.W., Quelle, D.E., 2005. Nucleophosmin (B23) targets ARF to nucleoli and inhibits its function. Mol. Cell. Biol. 25, 1258–1271.

Kucharski, T.J., Gamache, I., Gjoerup, O., Teodoro, J.G., 2011. DNA damage response signaling triggers nuclear localization of the chicken anemia virus protein Apoptin. J. Virol. 85, 12638–12649.

Kurki, S.P.K., Latonen, L., Kiviharju, T.M., Ojala, P.M., Meek, D., Laiho, M., 2004. Nucleolar protein NPM interacts with HDM2 and protects tumor suppressor protein p53 from HDM2-mediated degradation. Cancer Cell 5, 465–475.

Lambert, B., Buckle, M., 2006. Characterisation of the interface between nucleophosmin (NPM) and p53: potential role in p53 stabilisation. Febs. Lett. 580, 345–350.

Laptenko, O., Prives, C., 2006. Transcriptional regulation by p53: one protein, many possibilities. Cell Death Differ. 13, 951–961.

Lee, N., Ryu, H.G., Kwon, J.H., Kim, D.K., Kim, S.R., Wang, H.J., 2016. Sirt6 depletion suppresses tumor growth by promoting cellular senescence induced by DNA damage in hcc. PLoS One 11, e0165835.

Li, F.Q., Tam, J.P., Liu, D.X., 2007. Cell cycle arrest and apoptosis induced by the coronavirus infectious bronchitis virus in the absence of p53. Virology 365, 435–445.

Lindström, M.S., 2010. NPM1/B23: a multifunctional chaperone in ribosome biogenesis and chromatin remodeling. Biochem. Res. Int. 2011, 195209.

Liu, H., Teng, Y., Zheng, X., Wu, Y., Xie, X., He, J., Ye, Y., Wu, Z., 2012. Complete sequence of a viral nervous necrosis virus (NNV) isolated from red-spotted grouper (*Epinephelus akaara*) in China. Arch. Virol. 157, 77–82.

Low, C.F., Syarul, N.B., Chee, H.Y., Mzh, R., Najiah, M., 2017. Betanodavirus: dissection of the viral life cycle. J. Fish Dis. 40, 1489–1496.

Luo, Y., Chen, A.Y., Qiu, J., 2011. Bocavirus infection induces a DNA damage response that facilitates viral DNA replication and mediates cell death. J. Virol. 85, 133–145.

Mai, R.T., Yeh, T.S., Kao, C.F., Sun, S.K., Huang, H.H., Lee, Y.W., 2006. Hepatitis C virus core protein recruits nucleolar phosphoprotein B23 and coactivator p300 to relieve the repression effect of transcriptional factor YY1 on B23 gene expression. Oncogene 25, 448–462.

Mai, W.J., Liu, P., Wang, W.N., 2012. Characterization of the tilapia p53 gene and its role in chemical-induced apoptosis. Biotechnol. Lett. 34, 1797–1805.

Mai, W.J., Huang, F., Chen, H.Q., Zhou, Y.J., Chen, Y., 2016. Nervous necrosis virus capsid protein exploits nucleolar phosphoprotein Nucleophosmin (B23) function for viral replication. Virus Res. 230, 1–6.

Malumbres, M., Barbacid, M., 2009. Cell cycle, CDKs and cancer: a changing paradigm. Nat. Rev. Cancer 9, 153–166.

Mayer, C., Grummt, I., 2005. Cellular stress and nucleolar function. Cell Cycle 4, 1036–1038.

Möröy, T., Geisen, C., 2004. Cyclin E. Int. J. Biochem. Cell Biol. 36, 1424–1439.

Muller, L., Schaupp, A., Walerych, D., Wegele, H., Buchner, J., 2004. Hsp90 regulates the activity of wild type p53 under physiological and elevated temperatures. J. Biol. Chem. 279, 48846–48854.

Munday, B.L., Kwang, J., Moody, N., 2002. Betanodavirus infection of teleost fish: a review. J. Fish Dis. 25, 127–142.

Paladino, P., Marcon, E., Greenblatt, J., Frappier, L., 2014. Identification of herpesvirus proteins that contribute to G1/S arrest. J. Virol. 88, 4480.

Qin, Q.W., Wu, T.H., Jia, T.L., Hegde, A., Zhang, R.Q., 2006. Development and characterization of a new tropical marine fish cell line from grouper, *Epinephelus coioides* susceptible to iridovirus and nodavirus. J. Virol. Methods 58–64.

Qin, F.X., Shao, H.Y., Chen, X.C., Shi, T., Zhang, H.J., Miao, Z.Y., Wang, L., Chen, H., Zhang, L., 2011. Knockdown of NPM1 by RNA interference inhibits cells proliferation and induces apoptosis in leukemic cell line. Int. J. Med. Sci. 8, 287–294.

Reed, L.J., Muench, H., 1938. A simple method of estimating fifty per cent endpoints. Am. J. Epidemiol. 27, 493–497.

Roberts, J.M., Sherr, C.J., 2003. Bared essentials of CDK2 and cyclin E. Nat. Genet. 35, 8–10.

Rohaly, G., Korf, K., Dehde, S., Dornreiter, I., 2010. Simian virus 40 activates ATR-delta p53 signaling to override cell cycle and DNA replication control. J. Virol. 84, 10727–10747.

Russo, A., Russo, G., 2017. Ribosomal proteins control or bypass p53 during nucleolar stress. Int. J. Mol. Sci. 18, 140.

Sommerset, I., Nerland, A.H., 2004. Complete sequence of RNA1 and subgenomic RNA3 of Atlantic halibut nodavirus (AHNV). Dis. Aquat. Organ. 58, 117–125.

Su, Y.C., Chiu, H.W., Hung, J.C., Hong, J.R., 2014. Betanodavirus B2 protein induces hydrogen peroxide production, leading to Drp1-recruited mitochondrial fragmentation and cell death via mitochondrial targeting. Apoptosis 19, 1457–1470.

Tan, C., Huang, B., Chang, S.F., Ngoh, G.H., Munday, B., Chen, S.C., Kwang, J., 2001. Determination of the complete nucleotide sequences of RNA1 and RNA2 from greasy grouper (*Epinephelus tauvina*) nervous necrosis virus, Singapore strain. J. Gen. Virol. 82, 647–653.

Tollini, L.A., Frum, R.A., Zhang, Y., 2011. The role of the nucleolus in the stress response. The Nucleolus. Springer, New York, pp. 281–299.

Vogelstein, B., Lane, D., Levine, A.J., 2000. Surfing the p53 network. Nature 408, 307–310.

Yang, X.J., Liu, J., Ye, L., Liao, Q.J., Wu, J.G., Gao, J.R., She, Y.L., Wu, Z.H., Ye, L.B., 2006. HCV NS2 protein inhibits cell proliferation and induces cell cycle arrest in the S-phase in mammalian cells through down-regulation of cyclin A expression. Virus Res. 121, 134–143.

Yang, K., Wang, M., Zhao, Y., Sun, X., Yang, Y., Li, X., Zhou, A., Chu, H., Zhou, H., Xu, J., Wu, M., Yang, Y., Yi, J., 2016. A redox mechanism underlying nucleolar stress sensing by nucleophosmin. Nat. Commun. 7, 13599.

Yuan, X., Wu, J., Shan, Y., Yao, Z., Dong, B., Chen, B., 2006. Sars coronavirus 7a protein blocks cell cycle progression at g0/g1 phase via the cyclin d3/prb pathway. Virology 346, 74–85.

Zhang, Y., Lu, H., 2009. Signaling to p53: ribosomal proteins find their Way. Cancer Cell 16, 369–377.

Zimmerman, E.S., Sherman, M.P., Blackett, J.L., Neidleman, J.A., Kreis, C., Mundt, P., Williams, S.A., Warmerdam, M., Kahn, J., Hecht, F.M., 2006. Human immuno-deficiency virus type 1 Vpr induces DNA replication stress in vitro and in vivo. J. Virol. 80, 10407–10418.

Zou, T., Rao, J.N., Liu, L., Marasa, B.S., Keledjian, K.M., Zhang, A.H., Xiao, L., Bass, B.L., Wang, J.Y., 2005. Polyamine depletion induces nucleophosmin modulating stability and transcriptional activity of p53 in intestinal epithelial cells. Am. J. Physiol. Cell Physiol. 289, C686–696.